OPEN ACCESS

International
Journal
Of Modern Engineering Research (IJMER)

Numerical Analysis of Conjugate Cooling of Turbine Blades with Smooth Circular Cooling Passages

G Vivek Bharadwaj[1], Vijaya Raghu B[2], Panduranga B P[3]

[1](MTech Scholar, Mechanical Engineering Department, Maharaja Institute of Technology, Mysore, India)
[2, 3] (Professor, Mechanical Engineering Department, Maharaja Institute of Technology, Mysore, India)

***ABSTRACT**: Cooling of turbine blades is essential to achieve longer life under high compression ratios and high turbine entry temperatures. Geometry of cooling passages plays major role in effective cooling of blades with minimal pressure drops. Different cooling passage geometries involving smooth circular holes placed on chord line of the blade profile have been considered in this work. Numerical simulation of conjugate heat transfer to coolant air is carried out using commercial FLUENT software. Analysis is carried out to capture minimum pressure drop across the passages and mini-max local blade temperature under different geometrical configurations. Simulated results are compared for various circular passage geometries developed for same cooling passage area ratios as well as coolant air velocities. Similar analysis has also been carried out for different coolant passage perimeter ratios and mass flow rates. Various parameters like maximum blade temperature, pressure drop across the passages and average Stanton number have been observed and analyzed for the cases considered in this work. A non-dimensional maximum temperature has been used for the analysis to make the conclusions drawn independent of dimensions and conditions considered in this work. Development of hot spots is observed near the leading edge of the blade for all the passage geometries considered and coolant passage geometries having passage area concentrated towards the leading edge showed better temperature distribution and reduction in maximum blade temperature. Passage configurations with narrower and more in number of passages showed better cooling in area ratio based cases and similar explicit conclusions could not be drawn with perimeter based cases. Rather than distribution of total passage area or total passage perimeter among the number of passages, positioning of passages seems to play vital role in efficient cooling of blades.*

***Keywords:** Coolant passage Area ratio, Coolant passage Perimeter ratio, Conjugate cooling, Numerical simulation, Smooth circular passages, Turbine blade cooling.*

I. INTRODUCTION

In turbine industry lot of developments have been succeeded in the recent past years near the vicinity of power generation criteria using gas and steam turbines. It is highly imperative to keep turbine entry temperature of hot gas entering turbine in order attain high thermal efficiency and thereby effective and efficient cooling of blades gains the focus. Many researchers has discussed about conjugate cooling of gas turbine blades. In this work, 3-D numerical analysis of conjugate cooling of a stator blade of a gas turbine has been considered. Much used profile E580 has been chosen for the analysis. Various configurations of smooth circular coolant passages placed along the chord line of the blade have been considered. Numerical simulation of blade cooling was carried out for different coolant passage geometries. Modelling of blade was done by using CATIA® software and numerical simulation using ANSYS Workbench®. Different geometries have been formed by dividing the total coolant passage area among the number of circular passages placed along the chord line of the profile. Basically the interest of the work was to compare the cooling and temperature distribution for the different coolant passage configurations with same total passage area. Similarly, hole perimeter based cases were also developed by dividing total perimeter of cooling passage among the perimeters of number of circular holes. Parameters considered in present study were non-dimensional maximum temperature, average pressure drop along the coolant passages and average internal surface Stanton number. Area based cases were simulated for various inlet coolant velocities and perimeter based cases were simulated for various mass flow rates of coolant air.

Various researchers have analyzed similar cases of turbine blade cooling using numerical simulation. Many such literatures were reviewed and certain conditions were extracted to adopt in the methodology of this work. F Mendonça, J Clement, et al in their work have used C3X blade for analysis and implemented polyhedral mesh for both solid and liquid domain. They have compared the results simulated out of polyhedral mesh and hexahedral mesh for various parameters such as pressure drop, Mach number and mid span temperature of the

blade [1].Chandrakant R, Kini, SatishShenoy B et al in their work, had provided coolant passages on the chord line and they had implemented both helicoidal and circular shaped coolant passages. They have compared both coolant passage geometries for the surface temperature at mid span of the blade and concluded that helicoidal geometry provides better cooling but practical problems while fabrication of blades has to be explored [2**].** Mangesh Kane and SavasYavuzkurt et al in their presented work have cited an overview of the results of iterative conjugate heat transfer calculations of gas turbine blade temperatures obtained using FLUENT [2006] code. They had used unstructured mesh for 2d blade model in their analysis. They have concluded that 30% deviation is noticed in heat transfer coefficients between simulated result and experimental results. By their prediction this might be because of re-laminarization of flow at leading edge of blade which had not taken into account during simulating the case [3].Robert Kwiatkowski, Roman Doma´nski et al in their proposed article dealt with heat transfer problems encountered in the cooling of jet engine turbine blades with internal cooling only. They had found that heat transfer coefficient at leading edge to be 150 W/m^2K.They have concluded that film cooling is very much needed at the leading edge of the blade but feasibility of fabricating film cooling holes at leading edge is difficult as two external surfaces of the blade are very close to each other [4].

II. ABBREVIATIONS AND TERMINOLOGY

Following is the tabulation of abbreviations of the terms that are used in this current work (Table 1).

Table 1: Abbreviations and definitions

V_{in}	Velocity of coolant at the inlet of passage.
m_{in}	Coolant mass flow rate.
ΔP_{avg}	Average pressure drop along coolant passage.
T_{in}	Temperature of coolant at inlet of coolant passage
A_r	Area ratio is the ratio of total coolant passage area to area of the blade profile.
P_r	Perimeter ratio is the ratio of total coolant passage perimeter to perimeter of the blade profile.
h	Convective heat transfer coefficient.
D_{cp}	Diameter of coolant passage.
l_c	Characteristic length: It is given by area of blade profile divided the by chord length of blade profile. $\mathrm{lc} = \frac{\mathrm{A_p}}{l_{ch}}$
A_p	Area of the blade profile.
l_{ch}	Chord length of the blade profile.
ΔT_{max}	Difference between maximum blade temperature and minimum coolant temperature.
Non dimensional T_{max}	It is the ratio of heat diffused with maximum temperature difference per unit area to heat flux at the boundary. $\mathrm{Non-dimensional\ T_{max}} = \frac{k\Delta T_{max}}{q_{avg}\, l_c}$
St	Stanton number

III. COMPUTATIONAL DOMAIN AND BOUNDARY CONDITIONS

Computational models were created using commercial software CATIA® for blade profile E580 shown in Fig 1. Meshing has been done using ANSYS Workbench14® software. The whole computational domain is comprised of meshed solid domain in the blade material and meshed fluid flow domain in coolant passages placed along the chord line of the blade as shown in Fig 2. These two meshed domains were coupled at the interface walls.

To simulate to the blade cooling, different geometrical configurations of coolant passage were obtained under two considerations.

- Area based (A_r) cases.
- Perimeter based (P_r) cases.

In area based cases, respective total passage cross-sectional area obtained for area ratios ranging between 0.1 and 0.15 was divided among the number of circular passages. In these cases, velocity of coolant air at inlet was maintained same for all the passages in each case and varied from 90m/s to 140m/s. In perimeter based cases, respective total perimeter of coolant passage obtained for perimeter ratios ranging between 0.3 and 0.38 was divided among the perimeters number of circular passages. In these cases, mass flow rate of coolant air at inlet was maintained same for all the passages in each case and varied from 0.004m/s to 0.007m/s.

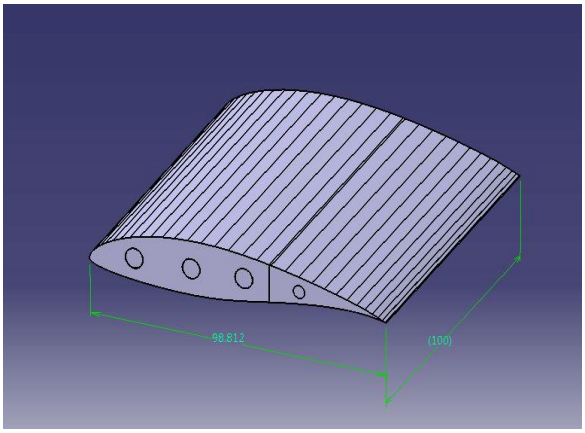

Figure1: three dimensional E580 blade with coolant passages (in mm)

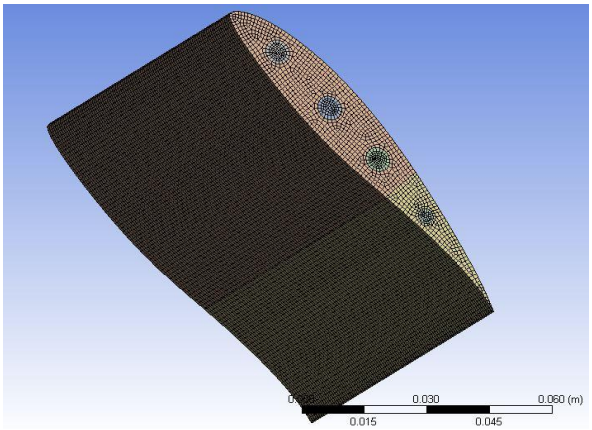

Figure 2: Meshed blade figure with 1,03, 000 elements.

Case 1: Obtained total coolant passage area for each area ratio was divided into 3 coolant passage of same areas and a 4 mm diameter hole near the trailing edge (Fig 3) all placed along the chord line.

Case 2: Obtained total coolant passage area for each area ratio was divided into 2 coolant passages of same areas and a 4 mm diameter hole is near the trailing edge (Fig 4) all placed along the chord line.

Case 3: Obtained total coolant passage area for each area ratio was divided between a 4mm diameter hole at the vicinity of trailing edge and rest of the area shared by 2 coolant passages in 2: 1 ratio (Fig 5) all placed along the chord line.

Case4: Configured similar to Case 2 with an additional coolant passage of diameter 5mm near the vicinity of the leading edge occupying its part of obtained total coolant passage area for each area ratio (Fig 6).

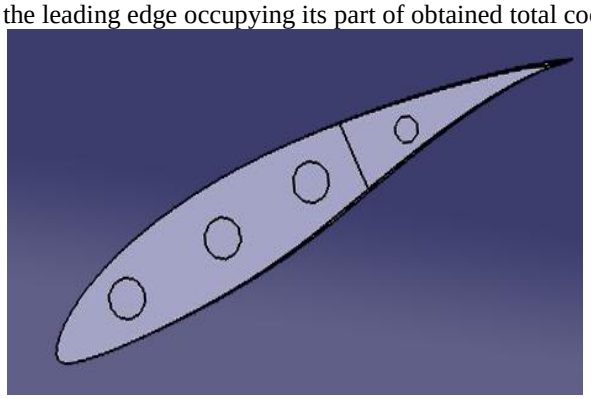

Figure 3: Case 1 for area ratio $A_r = 0.1$

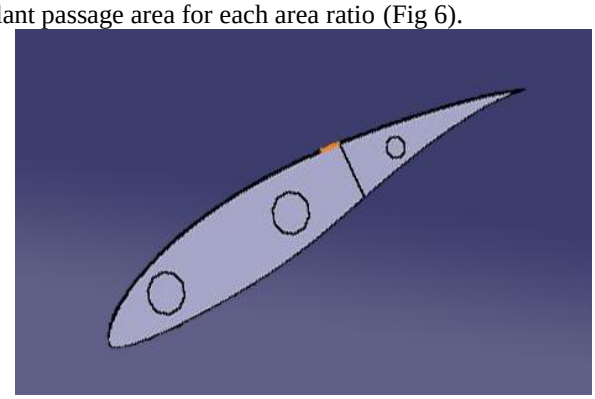

Figure 4: Case 2 for area ratio $A_r = 0.1$

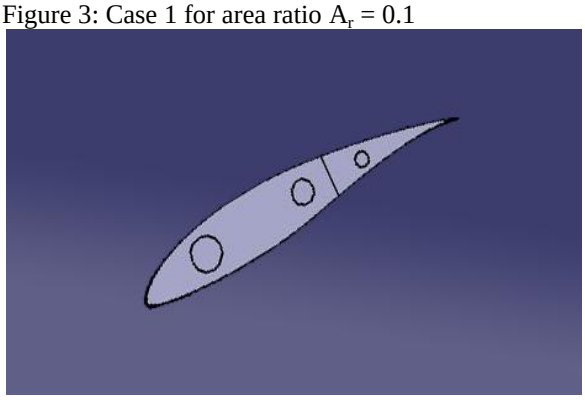

Figure 5: Case 3 for area ratio $A_r = 0.1$

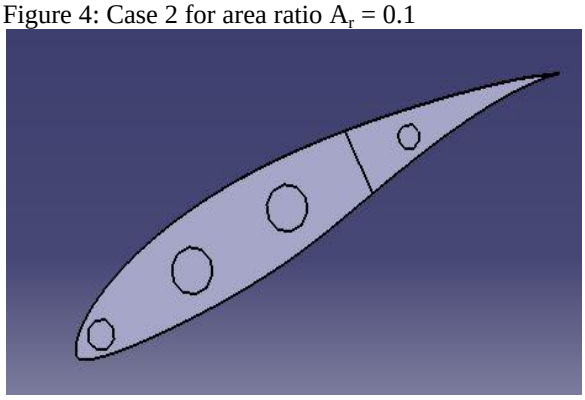

Figure 6: Case 4 for area ratio $A_r = 0.1$

Meshing was done using commercial Ansys Workbench 14® with unstructured hexahedral mesh for both solid and liquid domain setting growth rate to 2. In spacial discretisation, generally, refinement of mesh leads to decrease in truncation errors and increase in round-off errors. This leads to a requirement to strike balance between the errors with optimum grid density for consistent more accurate results [5]. Grid independence test was carried out to find near optimal grid density by simulating the problem starting from 32872 elements.

Further, problem was simulated several times with increase in the refinement of mesh. Variation in the results found minimal with the further refinement after number of elements crossed 1,03,000 shown in Fig 2.

Same grid density has been used for the meshing all the other cases considered in this study. Each case was subjected to different V_{in} and m_{in} for A_r and P_r cases respectively.

The coolant fluid is assumed to be incompressible with constant properties and the flow turbulent and steady. External surface of the blade was imposed with heat influx. Average magnitude of heat flux imposed on external blade surface was determined by simulating 2-D flow of hot gases over aerofoil with coolant holes applied with constant wall temperature condition. On the basis of flow separation near the tail, the blade was divided into 2 parts in 3:2 ratios from the leading edge. From the 2D simulation, averaged heat flux was extracted from the post processing in these two parts and applied as uniform heat flux boundary condition on the respective parts of outer surface of blades in all the cases. All numerical simulations are accomplished using finite-volume method. The boundaries of the computational domain include inlet, outlet and solid walls. A steady state unidirectional uniform velocities V_{in} was applied at inlet plane of coolant passage with T_{in} of 650K for the computations. At the outlet, pressure outlet condition was provided with gauge pressure set to null value. No-slip boundary condition was applied at the coolant passage surface. Zero heat flux boundary condition was applied at blade surfaces at the root and tip. Coolant properties and blade material properties set in this work were as per Table 2. Blade cooling involves strong currents of coolant through narrow passages and hence the influence of convection will be greater than the diffusion. On this basis, up wind scheme was found more suitable [6]. Standard k-ε turbulence model was employed to simulate the coolant flow across the passages.

Table2: Properties of coolant and blade material.

Parameters	Coolant fluid	Blade material
Density	0.6Kg/m^3	7950 Kg/m^3
Specific heat	1.6 KJ/Kg-K	436 KJ/Kg-K
Thermal conductivity	0.05(W/m-K)	11.5 (W/m-K)
Viscosity	$3.24 * 10^{-5}$Kg/m-s	

IV. RESULTS AND DISCUSSION

Above discussed cases were simulated for conjugate cooling for various inlet velocities and mass flow rates of coolant air. A_r based cases were simulated with coolant inlet velocities of 90, 100, 110, 120, 130 and 140m/s. Perimeter based cases were simulated with coolant mass flow rates of 0.004, 0.005, 0.006 and 0.007kg/s. In this present work cases of different A_r and P_r were subjected to simulation using standard k-ε turbulence model. Contours of static temperature for 0.1 A_r are shown in the Fig 7, 8, 9, 10 for all 4 cases respectively with V_{in} of coolant at 120m/s and T_{in} at 650K.

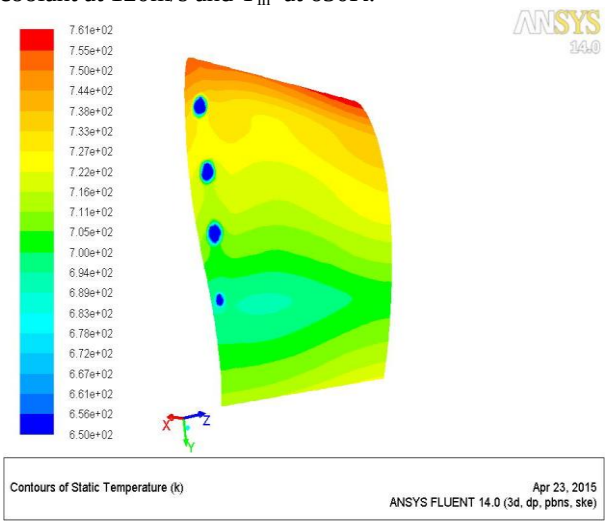

Figure 7: contour plot of static temperature distribution of Case 1 of A_r 0.1 ratio.

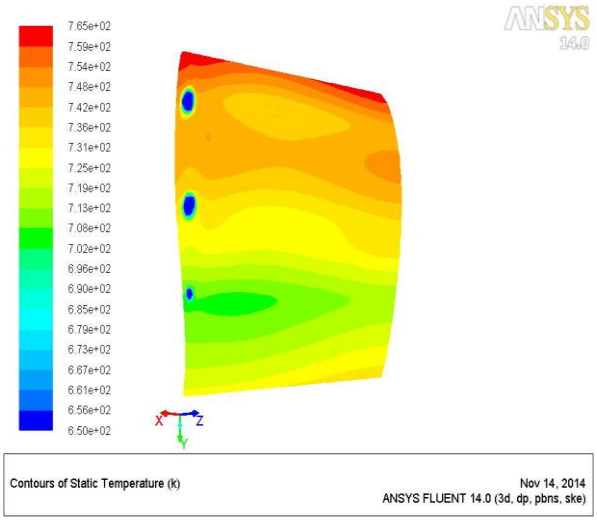

Figure 8: contour plot of static temperature distribution of Case 2 of A_r 0.1 ratio.

From the static temperature contours it is evident that hot spots are developed near the leading edge in all of the cases. Better temperature distribution can be observed in cases 1 and 4 when compared to cases 2 and 3. This can be perceived as total passage area divided among more number of holes leads to better degree of uniformity in temperature distribution rather than bigger and lesser number of holes. It can also be observed that higher temperature gradients are developed near the exit of smaller diameter passages. This may be attributed to lesser mass flow rates through smaller holes and hence lesser heat carrying capacity in area based cases.

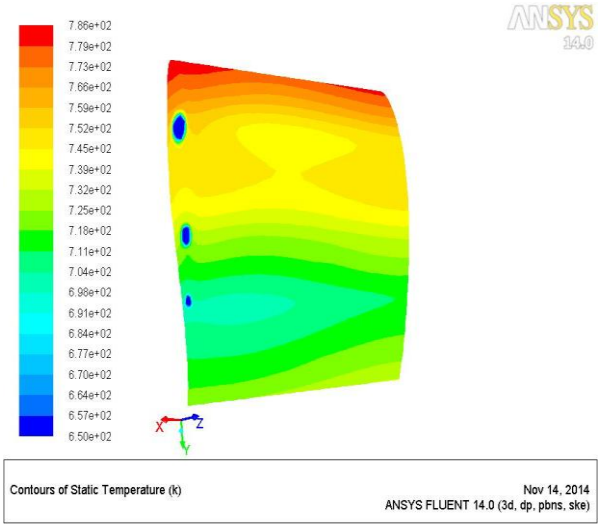

Figure 9: contour plot of static temperature distribution of Case 3 of A_r 0.1 ratio.

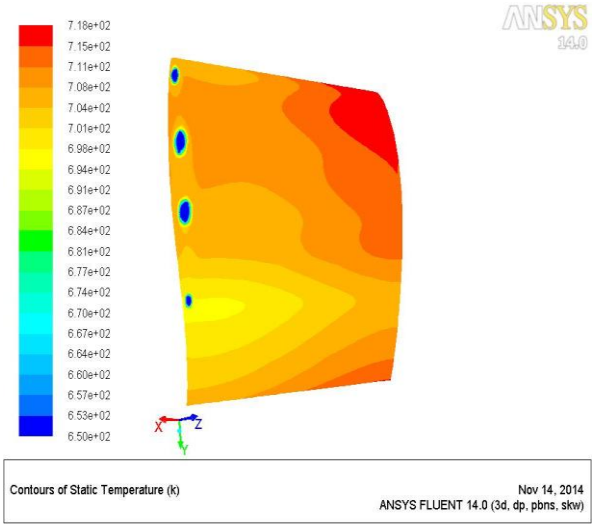

Figure 10: contour plot of static temperature distribution of Case 4 of A_r 0.1 ratio.

4.1 Passage area based cases for A_r = 0.08

Graphs 1(a), 1(b), 1(c) and 1(d) show the variation of various parameters with different passage configurations considered. It is evident that higher velocities result in reduction in maximum temperature and same trend is observed with all the passage configurations considered. From the plots it is clear that passage configuration used in case 4 provides better temperature distribution and leads to considerably lesser T_{max} than other cases and almost 50% lesser T_{max} compared to case 2. Understandably, higher coolant velocities leading to higher turbulence suffered increase in average pressure drops across the passages. Cases with narrow passages resulted in comparatively higher pressure drops. Case 4, having passage area concentrated towards leading edge resulted in lesser maximum temperature as hot spots tend to build up near leading edge. Case 1 with more uniformly distributed passage area showed decent cooling pattern but poor and higher average pressure drop.

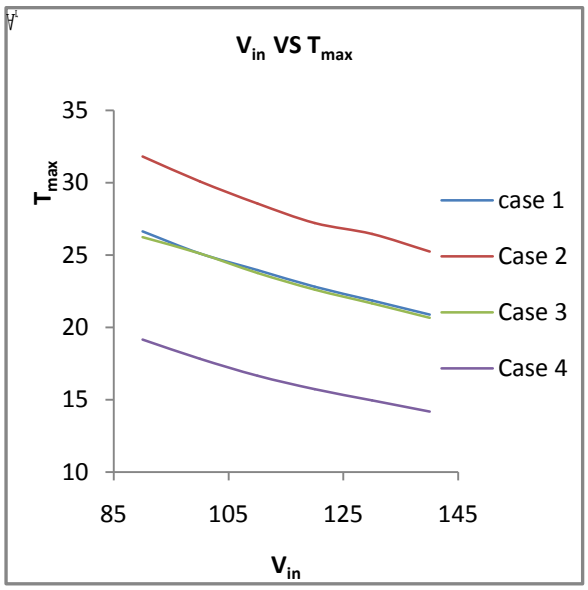

Graph 1(a): Variation of T_{max} with respect to V_{in}.

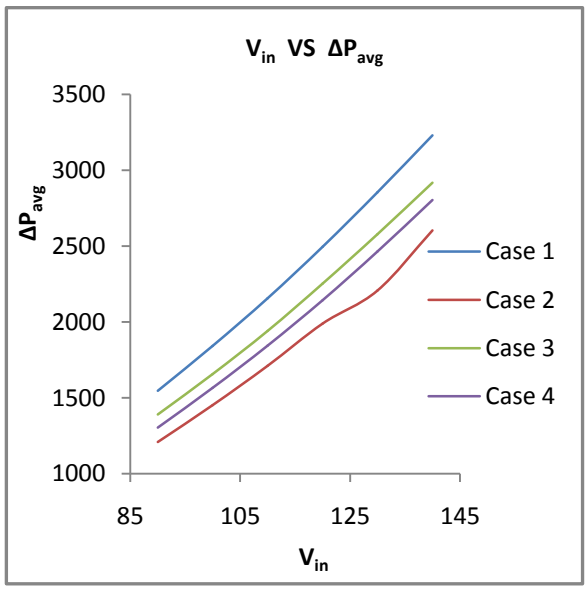

Graph 1(b): Variation of ΔP_{avg} with respect to V_{in}.

From the graph 1(c), it can be observed that, configurations with broader passages, case 2 and case 3 exhibited high convective conditions. This might be because of high degree of turbulence in broader passages leading to higher convective coefficient. Same argument holds well with the tendency of increase in St Number with the coolant velocity. It is also evident from Graph 1(d) that there is no explicit relation between St Number and temperature distributions, but the placement of passages plays the major role in effective cooling.

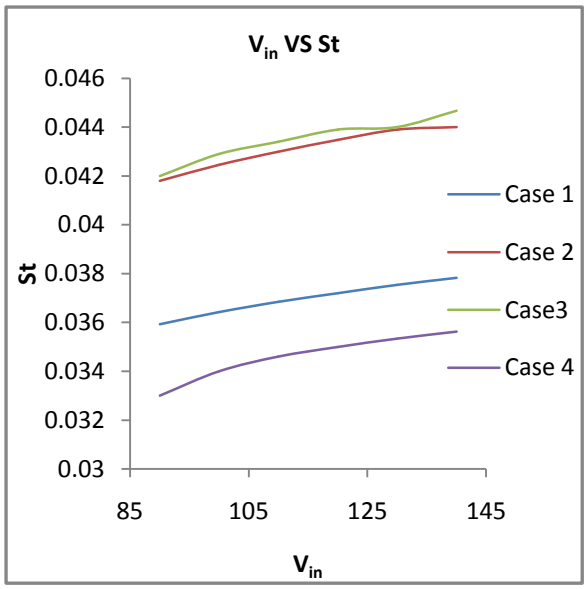

Graph 1(c): Variation of St with respect to V_{in}.

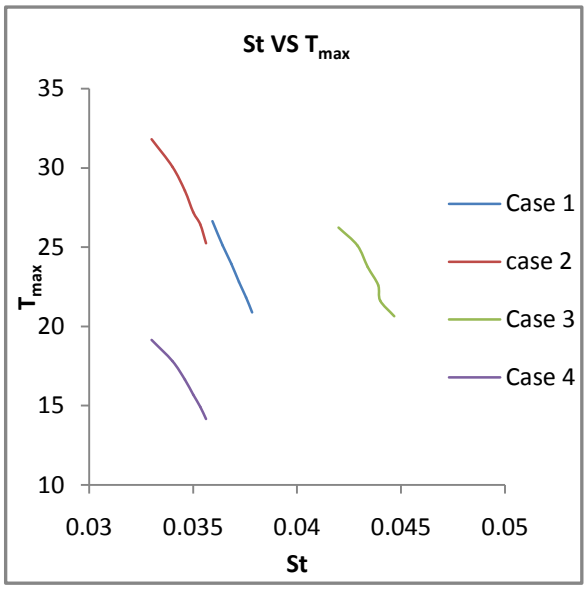

Graph 1(d): Variation of T_{max} with St.

4.2 Passage area based cases for Ar = 0.1

Graphs 2(a), 2(b), 2(c) and 2(d) show the variation of various parameters with different passage configurations considered. It can be observed from the plots that, with the increase in the area ratio, case 2, the more uniformly distributed passage configuration performed with better temperature distribution and reduced maximum temperature. As in the previous area ratio passage geometry case 4 came out best in terms of temperature distribution and reduction in maximum temperature. Cases with broader passages resulted with hot spots at higher temperatures. But, average pressure drop across the passages trend remains similar with increase in the area ratio. As in the previous area ratio, average St Number ranged with higher values for the cases with broader and less number of passages.

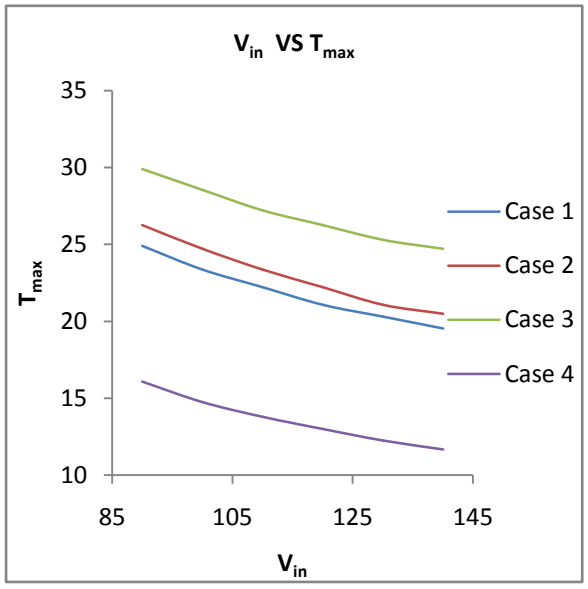

Graph 2(a): Variation of T_{max} with respect to V_{in}.

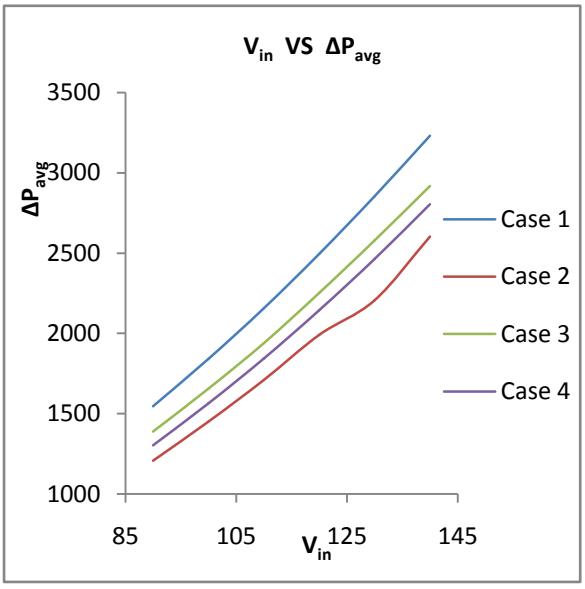

Graph 2(b): Variation of ΔP_{avg} with respect to V_{in}.

From the graph 2(d), it can be observed that configurations with more number of smaller passages exhibited better cooling even with lesser convective coefficients. This trend is might be because of total passage area shared by more number of passages allows larger heat transfer area for convection. And also the placement of passages has its role in effective cooling.

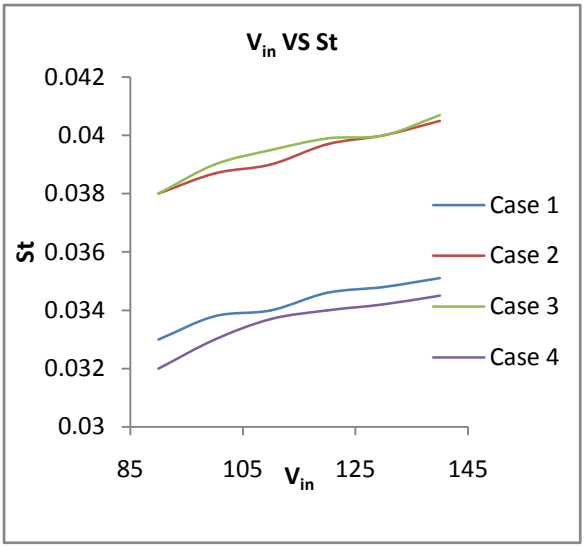

Graph 2(c): Variation of St with respect to V_{in}.

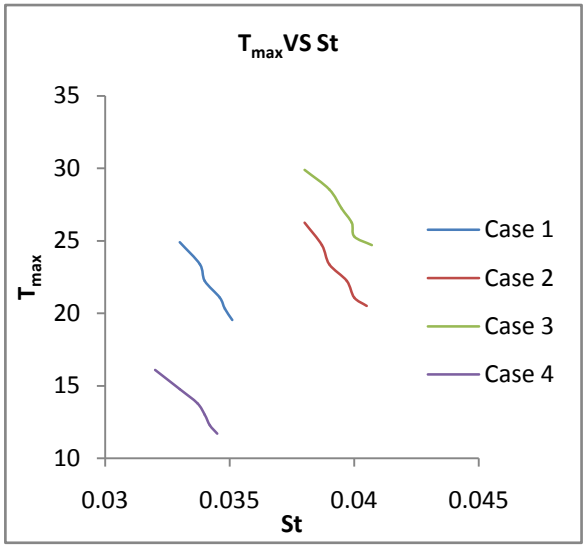

Graph 2(d): Variation of T_{max} with respect to St.

4.3 Passage area based cases for A_r = 0.15

Graphs 3(a), 3(b), 3(c) and 3(d) show the variation of various parameters with different passage configurations considered. In this area ratio also, as in the previous ratios, passage geometry case 4 performed better than the other geometries in terms of temperature distribution and reduction in maximum temperature. T_{max} variation was very similar comparing to previous cases of case 4. Average pressure drop trend remains same with increase in the area ratio. St Number was almost similar with the cases 1 and 4, both having more number of narrower passages along the blade chord line. Cases with lesser St Number exhibiting better cooling suggest that surface area for convection and position of passages play vital role than convective coefficient.

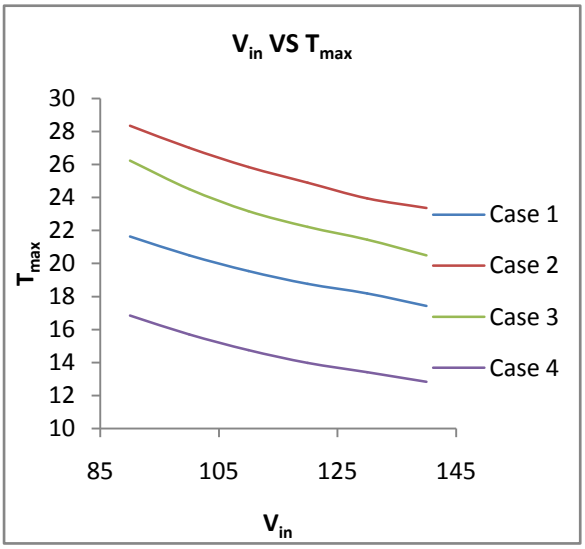

Graph 3(a): Variation of T_{max} with respect to V_{in}.

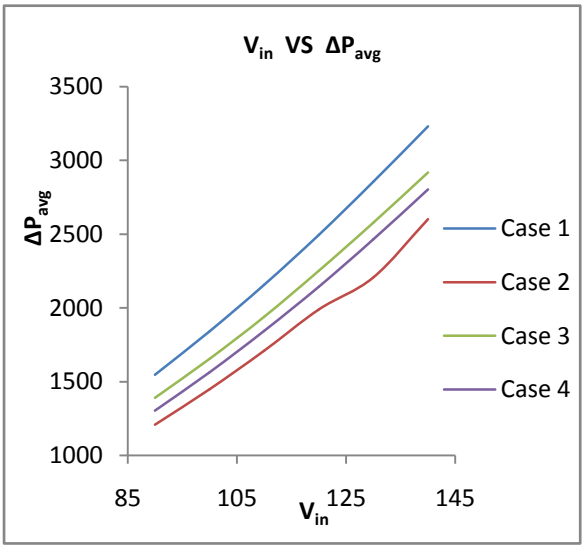

Graph 3(b): variation of ΔP_{avg} with respect to V_{in} .

From the graph 3(c), it can be observed that configurations with more number of smaller passages exhibited better cooling even with lesser convective coefficients. Case 1and Case 4 had closer convective coefficients compared with other cases and Case 1 provided better cooling in this area ratio when compared to previous area ratios. Graph 3(d) shows explicitly geometries with lesser St Number resulting in better cooling.

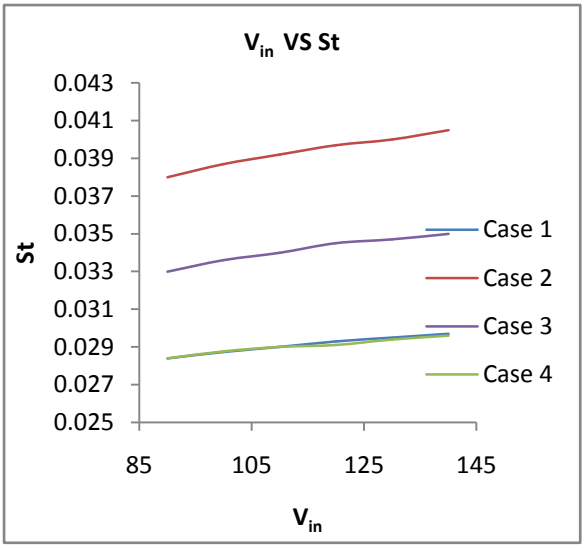

Graph 3(c): variation of St with respect to V_{in}

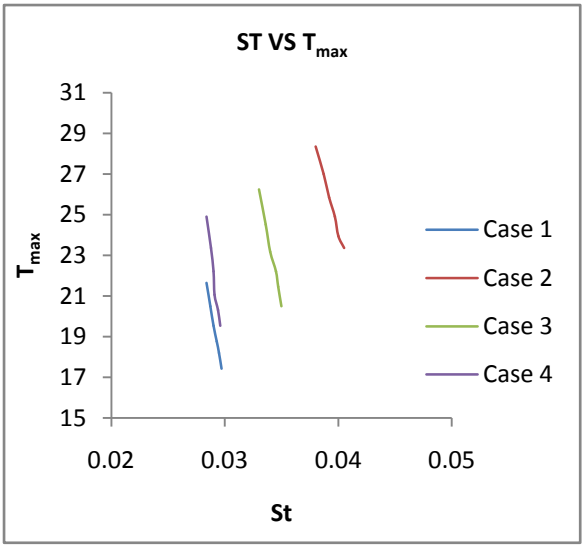

Graph 3(d): variation of T_{max} with respect to St.

4.4 Passage perimeter based cases for P_r = 0.30

Graphs 4(a), 4(b), 4(c) and 4(d) show the variation of various parameters with different perimeter based passage configurations considered. It is evident that higher mass flow rates results in reduction in maximum temperature and same trend is observed with all the passage configurations considered. From the plots it is clear that passage configuration used in case 4 provides better temperature distribution and leads to considerably lesser T_{max} than other cases. This clearly suggests that placement of passages has important role in efficient cooling. Cases having more number of passages for same total passage perimeter showed better cooling trends. Cases with narrow passages resulted in comparatively higher pressure drops and almost followed similar trend. Case 4, having passage area concentrated towards leading edge resulted in lesser T_{max} as hot spots tend to build up near leading edge. Case 1 with more uniformly distributed passage perimeter was almost having same pressure drop as that of case 4 but T_{max} was higher than the same.

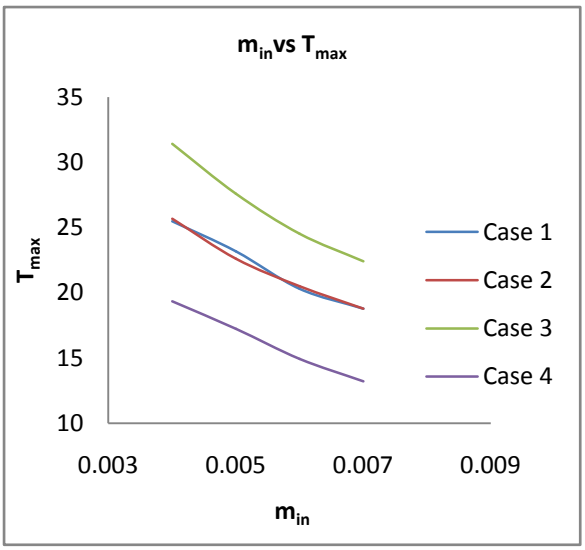

Graph 4(a): Variation of T_{max} with respect to m_{in}.

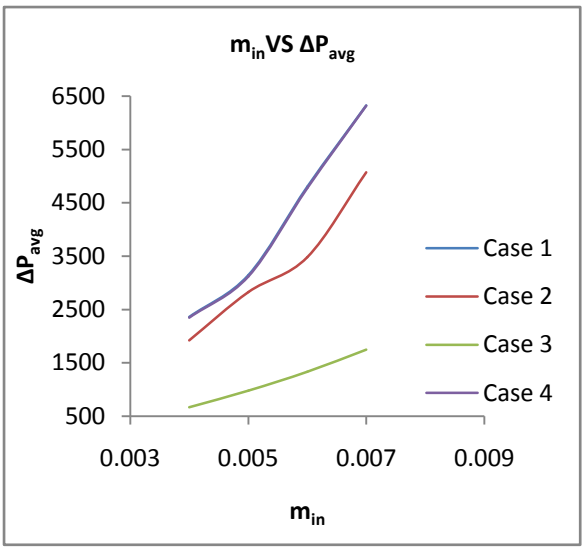

Graph 4(b): Variation of $\Delta P_{avg}$with respect to m_{in}

From the graph 4(c), it can be observed that, configurations with broader passages, case 2 and case 3 exhibited moderate convective conditions. Configurations with narrower passages showed steeper increase in convective coefficient with the increase in the mass flow rate. It is also evident from Graph 4(d) that case with combination of broader and narrower passages showed larger range of St Number and all other cases with evenly distributed passages showed almost same trend and has similar T_{max} variation.

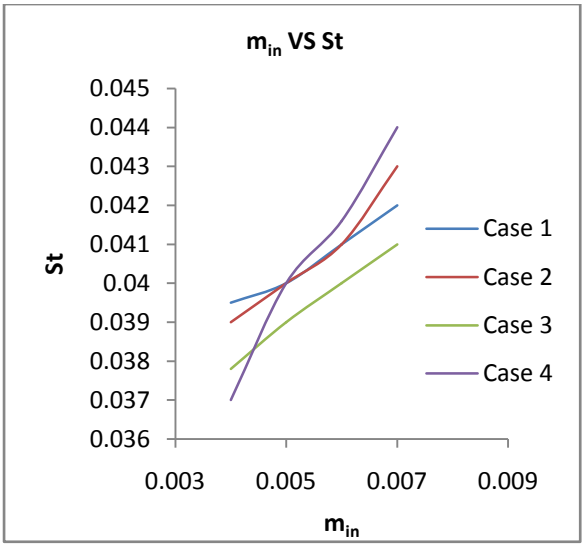

Graph 4(c): Variation of St with respect to m_{in}

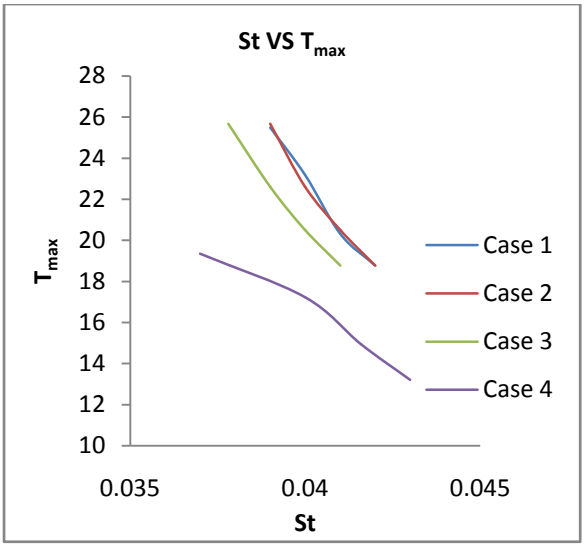

Graph 4(d): variation of T_{max} with respect to St.

4.5 Passage perimeter based cases for P_r = 0.34

Graphs 5(a), 5(b), 5(c) and 5(d) show the variation of various parameters with different perimeter based passage configurations considered. As in the previous perimeter ratio, case 4 performed better than other cases even for this perimeter ratio in terms of temperature distribution and maximum temperature. Case 1, configuration with more uniformly distributed passages performed better than that of in previous perimeter ratio. Even though area available for convection in passages has significantly increased, no significant improvement in cooling is observed in configurations with broader passages. But, cooling has improved in configurations with narrower passages with increase in the perimeter ratio. Increase in the perimeter ratio for same mass flow rates has reduced the pressure drop significantly. Following the similar trend of configurations and conditions discussed earlier, case with broader passages showed least pressure drop across the passages. In contrast with the area based cases, case 1 exhibited higher average St Number and moderate cooling in perimeter based cases. As total mass flow rates are kept same for perimeter based cases, configurations with broader passages did not show higher St Numbers.

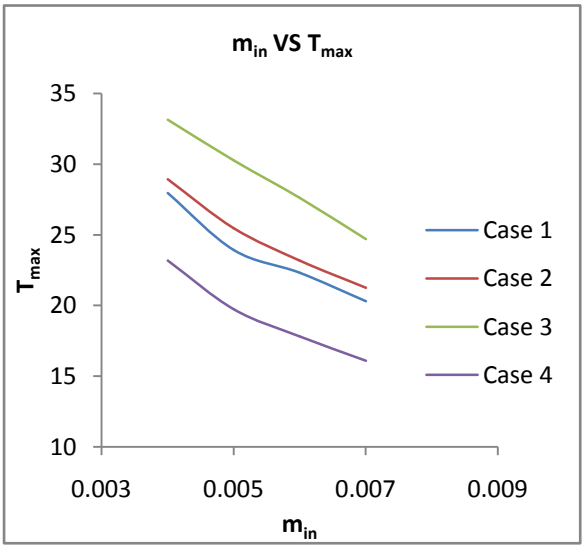

Graph 5(a): Variation of T_{max} with respect to m_{in}.

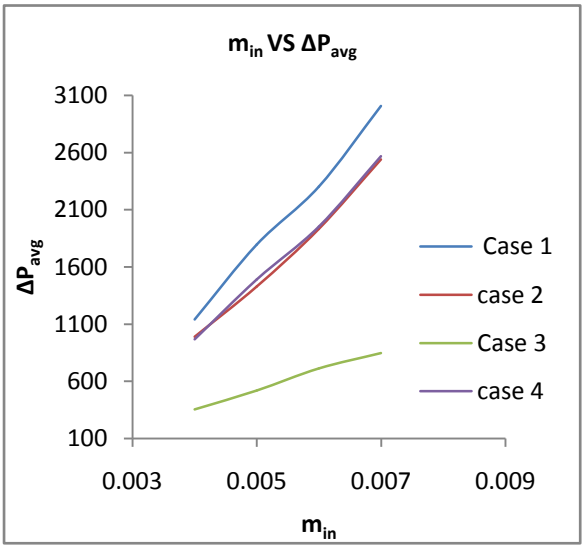

Graph 5(b): Variation of $\Delta P_{avg}$with respect to m_{in}.

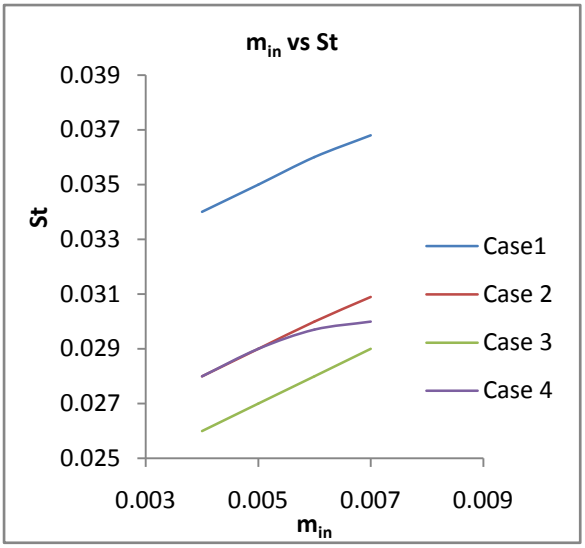

Graph 5(c): Variation of St with respect to m_{in}.

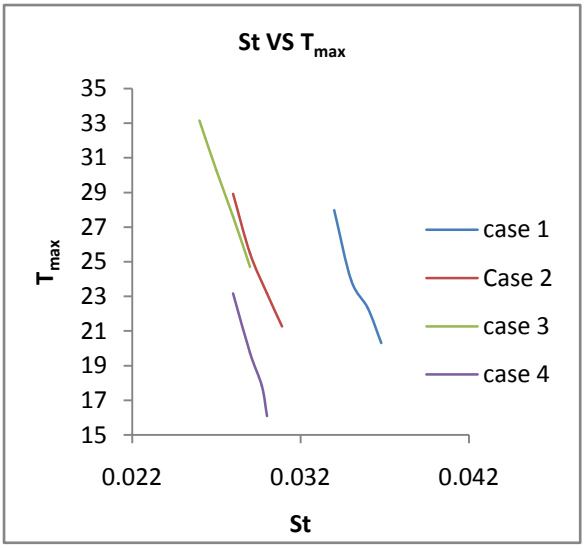

Graph 5(d): Variation of T_{max} with respect to St.

4.6 Passage perimeter based cases for P_r = 0.38

Graphs 6(a), 6(b), 6(c) and 6(d) show the variation of various parameters with different perimeter based passage configurations considered. As in the previous perimeter ratios, case 4 performed better than other cases even for this perimeter ratio in terms of temperature distribution and maximum temperature. Passage geometries with narrower and more in number of passages showed considerable reduction in maximum temperature when compared with geometries with broader passages as in previous cases. Except case 4, all cases showed steep increase in pressure drops across with mass flow rates. Case 1, the configuration with more uniformly distributed passages got far from better performing configuration case 4 in terms of maximum blade temperature but resulted in high pressure drops in contrast with previous cases of lesser perimeter ratios. No explicit understanding can be drawn on effect of St Number on maximum temperature from graphs 6(c) and 6(d) as configurations exhibiting extreme St Numbers performed comparatively closer in terms of maximum blade temperature. This leads to the requirement of detailed study about the positioning of passages. Geometries with broader passages resulted with lesser St Numbers and hence lesser convective coefficients. This might be because of broader passages had lesser coolant velocities as these cases are mass flow rate based.

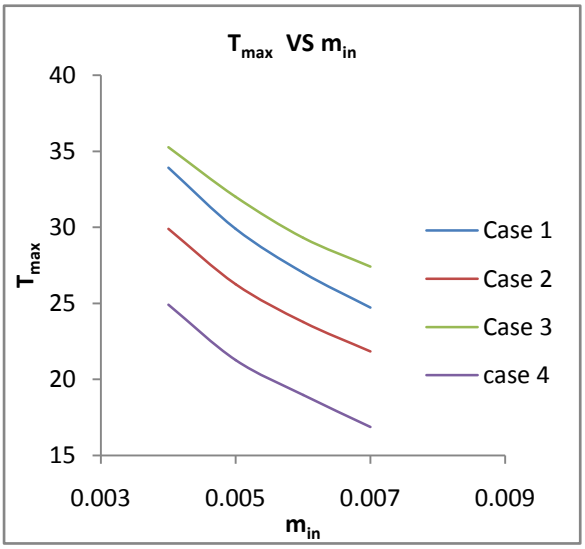

Graph 6(a): Variation of T_{max} with respect to m_{in}.

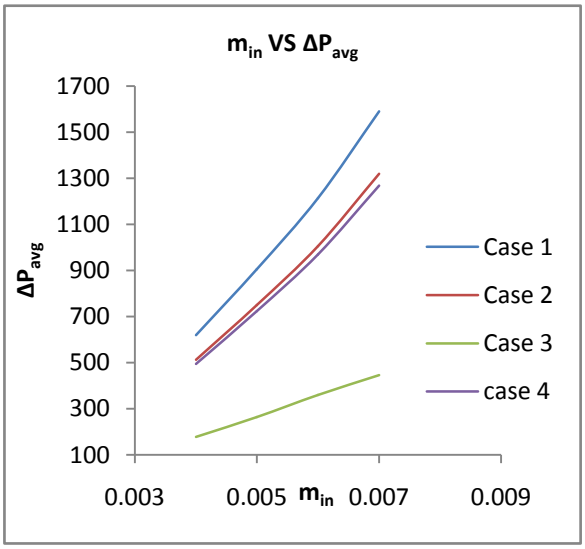

Graph 6(b): Variation of ΔP_{avg} with respect to m_{in}.

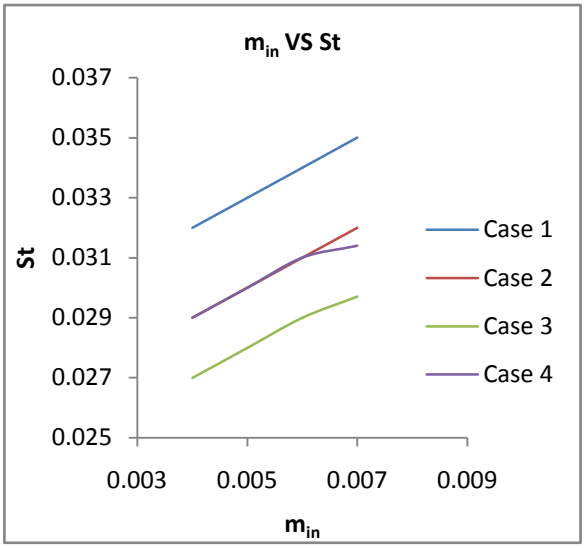

Graph 6(C): Variation of St with respect to m_{in} .

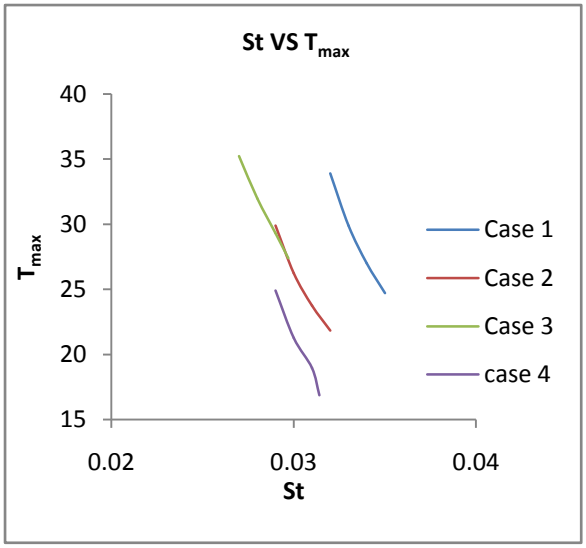

Graph 6(d): Variation of T_{max} with respect to St.

V. CONCLUSION

For all configurations based on both area ratio and perimeter ratio, maximum temperature occurred near the leading edge of the blade and varied inversely with velocity as well as mass flow rate of the coolant throughout the range considered. Blade surface reached higher temperatures near the exit of the passages when compared to inlet. Passage configurations with narrower passages resulted in higher pressure drops across the passages. Pressure drops increased with increase in coolant velocity and mass flow rate in respective cases. In area ratio based cases, even though configurations with broader passages showed higher convective coefficients due to higher turbulence, they did not resulted in better cooling patterns. In perimeter ratio based cases, configurations with more number of narrower passages showed better cooling but differed in St Number to the extremes. In general, configuration with broader passages at the mid of the chord line a passage near the leading exhibited better cooling with moderate pressure drops than other configurations considered irrespective of coolant flow conditions. It can be extracted from the results that distribution of total coolant passage area among passages effects most the coolant pumping power required and placement of passages effects the cooling pattern the most.

REFERENCES

Journal Papers:

[1] F. Mendonça, J. Clement and D. Palfreyman A. Peck "Validation of unstructured CFD modeling applied to the c3x turbine including conjugate heat transfer".

[2] Chandrakant R Kini, Satish Shenoy B and N Yagnesh Sharma "Numerical Analysis of Gas Turbine HP Stage Blade Cooling with New Cooling Duct Geometries", Proceedings of the World Congress on Engineering 2011 Vol III ,WCE 2011, July 6 - 8, 2011, London, U.K.

[3] Mangesh Kane and Savas Yavuzkurt "Calculation of gas turbine blade temperatures using an iterative conjugate heat transfer approach", Int. Symp. on Heat Transfer in Gas Turbine Systems 9*14 August 2009, Antalya, Turkey.

[4] Robert Kwiatkowski, Roman Doma´nski "Numerical analyses of heat transfer in high-temperature loaded turbine blades", Journal of Power Technologies 92 (4) (2012) 208–213.

Books:

[5] John D Anderson Jr "*Computational Fluid Dynamics-The Basics With Applications*" McGraw-Hill, Inc., New York, ISBN 0-07-001685-2.

[6] Versteeg H K., Malalasekera W., 1998 "An *Introduction to Computational Fluid Dynamics the Finite Volume Method"*, Second Edition, Pearson Education Limited, Essex, England (2007).